Regulation of axon repulsion by MAX-1 SUMOylation and AP-3

Shih-Yu Chen[a], Chun-Ta Ho[b], Wei-Wen Liu[b], Mark Lucanic[a], Hsiu-Ming Shih[c], Pei-Hsin Huang[b,1], and Hwai-Jong Cheng[a,d,1]

[a]Center for Neuroscience, University of California, Davis, CA 95618; [b]Graduate Institute of Pathology, College of Medicine, National Taiwan University, Taipei 10048, Taiwan; [c]Institute of Biomedical Sciences, Academia Sinica, Taipei 11529, Taiwan; and [d]Graduate Institute of Mind and Brain Sciences, College of Medicine, National Taiwan University, Taipei 10048, Taiwan

Edited by Kang Shen, Stanford University, Stanford, CA, and accepted by Editorial Board Member Yuh Nung Jan July 18, 2018 (received for review March 14, 2018)

During neural development, growing axons express specific surface receptors in response to various environmental guidance cues. These axon guidance receptors are regulated through intracellular trafficking and degradation to enable navigating axons to reach their targets. In *Caenorhabditis elegans*, the UNC-5 receptor is necessary for dorsal migration of developing motor axons. We previously found that MAX-1 is required for UNC-5–mediated axon repulsion, but its mechanism of action remained unclear. Here, we demonstrate that UNC-5–mediated axon repulsion in *C. elegans* motor axons requires both *max-1* SUMOylation and the AP-3 complex β subunit gene, *apb-3*. Genetic interaction studies show that *max-1* is SUMOylated by *gei-17/PIAS1* and acts upstream of *apb-3*. Biochemical analysis suggests that constitutive interaction of MAX-1 and UNC-5 receptor is weakened by MAX-1 SUMOylation and by the presence of APB-3, a competitive interactor with UNC-5. Overexpression of APB-3 reroutes the trafficking of UNC-5 receptor into the lysosome for protein degradation. In vivo fluorescence recovery after photobleaching experiments shows that MAX-1 SUMOylation and APB-3 are required for proper trafficking of UNC-5 receptor in the axon. Our results demonstrate that SUMOylation of MAX-1 plays an important role in regulating AP-3–mediated trafficking and degradation of UNC-5 receptors during axon guidance.

axon guidance | MAX-1 SUMOylation | AP-3 complex | UNC-5 receptor | *C. elegans*

A functional nervous system requires proper formation of neuronal connections, which begins with axon guidance (1). During this process, the growing axon is directed by various attractive and repulsive environmental cues until its tip, called the growth cone, reaches its final target. The guidance information is received by receptors on the growth cone, triggering a series of intracellular signals that move the axon in the correct direction. The diversity of developing axonal connections is established through dynamic regulation of environmental cues, surface receptors, and intracellular signaling networks (1, 2).

During dorsal guidance of developing motor axons in *Caenorhabditis elegans*, the UNC-5 receptor is expressed on axonal growth cones, which are then repelled by a gradient of UNC-6/Netrin in the environment (3–5). Accumulating evidence suggests that axon guidance requires proper trafficking and distribution of the UNC-5 receptors and its coreceptors UNC-40/DCC (6–9).

We previously isolated *max-1* (motor axon guidance-1) in a forward genetic screen and showed that *max-1* works with *unc-5* to regulate repulsion of motor axons in *C. elegans* (10). A subsequent genetic study in zebrafish also suggested that *max-1* plays a role in regulating membrane localization of Ephrin3b proteins, which provide guidance cues for the migration of intersegmental venous endothelial cells during embryogenesis (11). However, how *max-1* functions in the growth cone during *unc-5*–mediated axon repulsion is not clear. To address this issue, we used yeast two-hybrid screens to identify molecules that interact with MAX-1 and UNC-5.

The MAX-1–interacting protein GEI-17/PIAS1 is a SUMOylation E3 ligase (12). Protein SUMOylation is a posttranslational modification process that alters the activity, stability, and subcellular localization of the substrate protein (13). The dynamic and reversible features of SUMOylation make it an ideal biochemical switch to modulate diverse cellular processes, including segregation of chromosomes, repair of damaged DNA, regulation of transcription and enzyme activities, and control of intracellular trafficking (14, 15). SUMOylation is also involved in various aspects of neural development, which include proliferation, differentiation, apoptosis, target selection, synaptogenesis, and synaptic plasticity (16–21). Here we show that SUMOylation also plays a role in axon guidance by demonstrating that MAX-1 is a substrate of GEI-17/PIAS1 and that SUMOylation of MAX-1 is essential for UNC-5–mediated axon repulsion.

Our screen also identified an UNC-5–interacting protein, APB-3, the β subunit of the AP-3 complex, which is located in the plasma membrane, Golgi complex, and endolysosomal compartments. The AP-3 complex functions as an adaptor for trafficking cargo proteins and mediating protein degradation (22, 23). Studies in cultured neurons and in AP-3–deficient animals showed that AP-3 is involved in synaptic vesicle formation from tubular endosomes (24, 25) and may play a role in trafficking proteins within neuronal processes (26, 27). A recent

Significance

During neural development, growing axons navigate over long distances to reach their targets. A critical step in this process is the regulation of its surface receptors on the axon's growth cone in response to environmental cues. We focus on how the UNC-5 receptor in *Caenorhabditis elegans* motor axons is regulated during axon repulsion. By combining *C. elegans* genetics, biochemistry, and imaging, we found that MAX-1 SUMOylation and AP-3 complex have significant roles in UNC-5–mediated axon repulsion. Our findings reveal how SUMOylation and AP-3–mediated trafficking and degradation interact to help the growing axon find its final target.

Author contributions: P.-H.H. and H.-J.C. designed research; S.-Y.C., C.-T.H., W.-W.L., M.L., and H.-M.S. performed research; S.-Y.C., C.-T.H., W.-W.L., M.L., H.-M.S., P.-H.H., and H.-J.C. analyzed data; and S.-Y.C., P.-H.H., and H.-J.C. wrote the paper.

The authors declare no conflict of interest.

This article is a PNAS Direct Submission. K.S. is a guest editor invited by the Editorial Board.

[1]To whom correspondence may be addressed. Email: phhuang@ntu.edu.tw or hjcheng@ucdavis.edu.

This article contains supporting information online at www.pnas.org/lookup/suppl/doi:10.1073/pnas.1804373115/-/DCSupplemental.

Published online August 13, 2018.

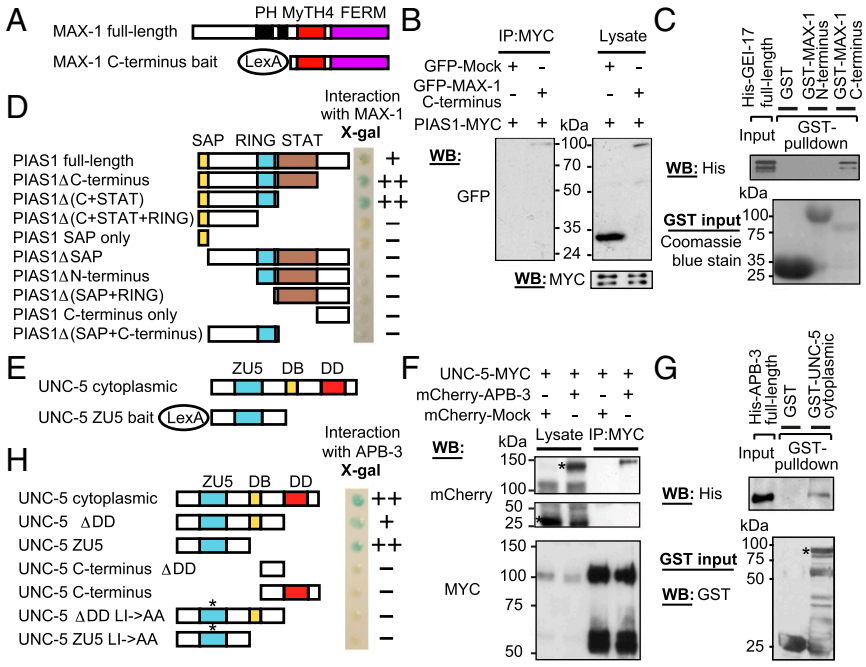

Fig. 1. Isolation of GEI-17/PIAS1 and APB-3 as MAX-1– and UNC-5–interacting proteins, respectively. (*A*) Schematic diagrams of the full-length mouse MAX-1 and the bait for yeast two-hybrid screen. MAX-1 contains two PH domains, an MyTH4 domain, and a FERM domain. The bait consists of LexA fused to the C terminus of MAX-1. FERM, band 4.1/ezrin/radixin/moesin; MyTH4, myosin tail homology 4; PH, pleckstrin homology. (*B*) Immunoblots show that GFP-MAX-1 coimmunoprecipitates with PIAS1. In comparison, GFP-mock did not form protein complex with PIAS1. (*C*) The C terminus of MAX-1, but not the N terminus, binds directly to GEI-17 in the GST pull-down assay. Note that the loading input is 5% of the total protein lysate. (*D*) Domain mapping by yeast two-hybrid assay indicates that the N-terminal half of PIAS1, which includes SAP and RING finger domains, is required for its interaction with MAX-1. Shown is a strip of representative X-gal reactions for yeast cells transformed with the indicated construct prey plus the MAX-1 C terminus bait. RING, really interesting new gene; S/T, serine- and threonine-rich; SAP, SAF-A/B, acinus and PIAS. (*E*) Schematic diagrams of the cytoplasmic region of UNC-5 and the ZU5 bait for yeast two hybrid screen. DB, DCC-binding; DD, death domain; ZU5, zona pellucida UNC-5. (*F*) APB-3, not the mock-control, is detected in the protein complex immunoprecipitated by MYC-tagged UNC-5. Asterisks indicate the mCherry-mock and mCherry-APB-3 bands in the lysates. (*G*) The cytoplasmic region of UNC-5 binds directly to the purified APB-3 in the in vitro GST pull-down assay. The loading input is 5% of the total protein lysate and the GST-UNC-5 cytoplasmic band in the input is indicated by an asterisk. (*H*) Domain mapping by yeast two-hybrid assay shows the UNC-5 ZU5 domain is sufficient for its interaction with APB-3. Mutations of both amino acids L(524)I(525) to A(524)A(525) in the ZU5 domain (asterisk) disrupt the interaction. A representative strip of X-gal reactions is shown for yeast cells transformed with indicated UNC-5 cytoplasmic construct tagged with LexA plus APB-3 full-length fused to GAL4AD.

report in *C. elegans* further demonstrates that AP-3 is required for differential targeting of transmembrane proteins into axons (28).

Here we report that UNC-5 interacts with APB-3 and that SUMOylated MAX-1 requires APB-3 to affect UNC-5–mediated axon repulsion. UNC-5 is degraded mainly in the endolysosomal compartment when APB-3 is overexpressed, and the interaction of UNC-5 and MAX-1 is significantly reduced in the presence of APB-3. We also show that the trafficking of UNC-5 receptors in axons requires SUMOylated MAX-1 and APB-3. Together, our results suggest that MAX-1 SUMOylation and the AP-3 complex play important roles in regulating the trafficking and degradation of UNC-5 receptors during axon guidance.

Results

GEI-17/PIAS1 and APB-3 Interact with MAX-1 and UNC-5, Respectively. In a yeast two-hybrid screen using the C terminus of mouse MAX-1 ortholog as bait (Fig. 1*A*), we isolated 16 independent positive colonies. Among these, two encoded fragments of mouse protein inhibitor of activated STAT-1 (PIAS1). The interaction of MAX-1 and PIAS1 was confirmed by coimmunoprecipitation from cotransfected COS cell lysates (Fig. 1*B*) and by pull-down of GST-tagged *C. elegans* MAX-1 with in vitro-purified *C. elegans* PIAS1 ortholog, GEI-17 (Fig. 1*C*). PIAS1 contains an SAF-A/B, acinus, and PIAS (SAP) domain in the N terminus, a really interesting new gene (RING) finger domain in the middle, and a less-conserved C terminus. Domain mapping showed that the N-terminal half, which includes SAP and RING domains, is necessary and sufficient for PIAS1's interaction with MAX-1 (Fig. 1*D*). The direct binding of MAX-1 to GEI-17/PIAS1 suggests MAX-1 could be a SUMOylation substrate regulated by GEI-17/PIAS1.

The cytoplasmic region of UNC-5 contains a zona pellucida UNC-5 (ZU5) domain, a DCC-binding (DB) domain, and a death domain (DD) (Fig. 1*E*). Because bait consisting of the entire UNC-5 cytoplasmic domain was self-activating, only the ZU5 domain was used as bait (labeled as UNC-5-ZU5) in the yeast two-hybrid screen for UNC-5 interacting molecules, which identified APB-3, the β subunit of AP-3 complex. Binding of UNC-5 with APB-3 into a protein complex was confirmed by coimmunoprecipitation and subcellular colocalization in cotransfected COS cells (Fig. 1*F* and *SI Appendix*, Fig. S1*A*) and by in vitro GST pull-down assay (Fig. 1*G*). Mapping for protein–protein interaction sites further revealed that a potential AP-binding dileucine motif of the ZU5 domain is responsible for UNC-5's binding with APB-3 (Fig. 1*H*). Given that APB-3 is an essential subunit of the tetrameric AP-3 complex, which regulates the sorting of vesicles mainly in the endolysosomal pathway (27, 29), the interaction of UNC-5 with APB-3 suggests that UNC-5 could be a cargo regulated by AP-3 for some sort of intracellular vesicular trafficking.

***gei-17* Functions Upstream of *max-1* to Regulate *unc-5*–Mediated Axon Repulsion.** In *C. elegans*, *gei-17* is involved in various cellular processes, including chromosome congression and telomere

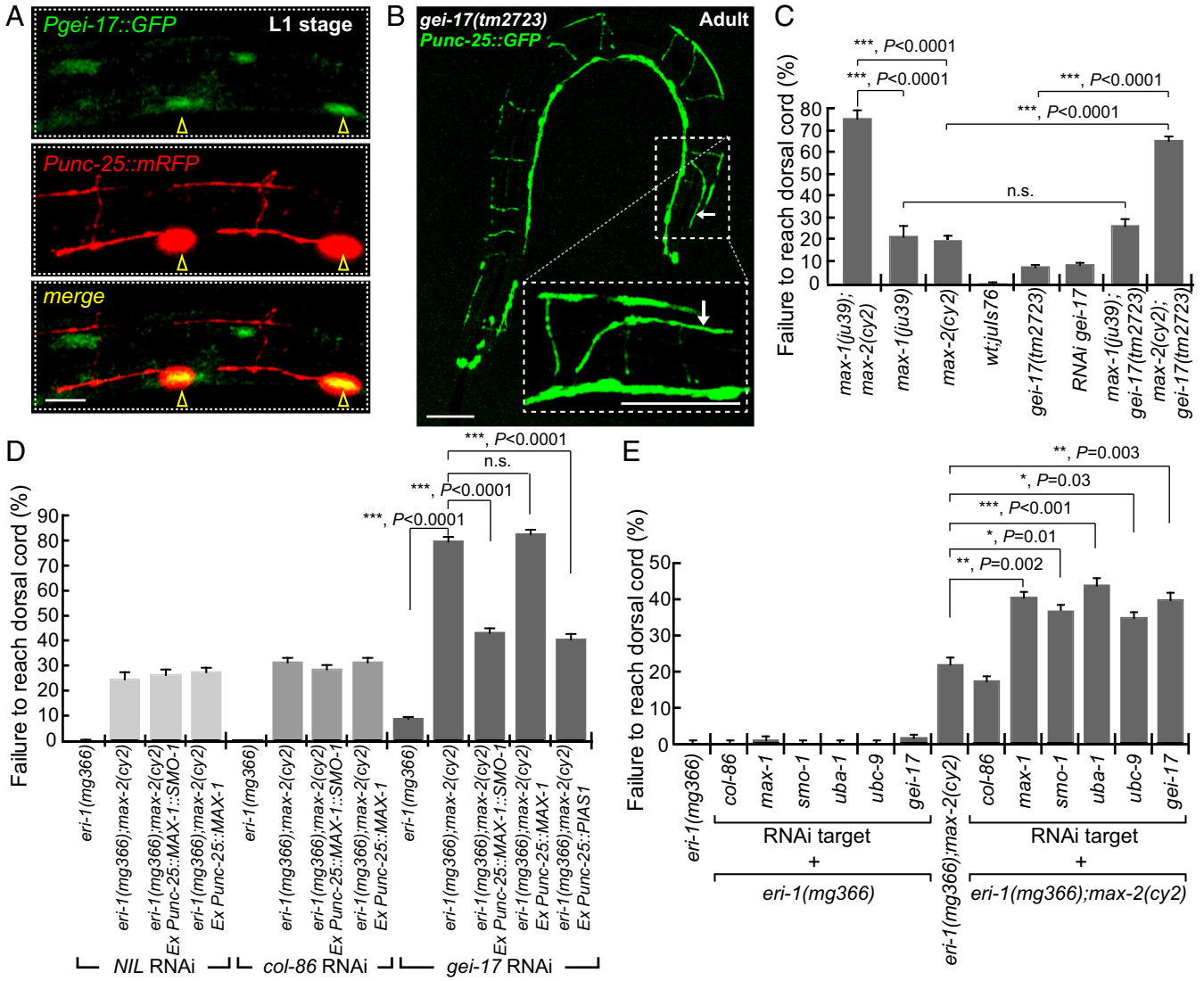

Fig. 2. *C. elegans gei-17* plays a role in the dorsal guidance of motor commissural axons. (*A*) *gei-17* is expressed in developing ventral cord motor neurons. At L1 stage, monomeric RFP driven by *unc-25* promoter is expressed strongly in DD neurons. GFP expression driven by the *gei-17* promoter is observed in the same neurons. Anterior is to the left and dorsal is up. (Scale bar: 5 μm.) (*B*) Some motor commissural axons are misguided in *gei-17(tm2723)* mutants (arrow) in the *juIs76[Punc-25::GFP]* background. (Scale bars: 20 μm.) (*C*) Quantification of axon guidance defects in *gei-17*, *max-1*, and *max-2* mutants. *gei-17* mutants exhibit mild guidance defects, and the mutation does not enhance effects of the *max-1* mutation. However, the defects of *max-2* mutants are significantly enhanced by the *gei-17* mutation. (*D*) Quantification of genetic interactions between *gei-17* and *max-1* with or without SUMOylation. SUMOylation mimetic WT *max-1* cDNA (*Ex Punc-25::MAX-1::SMO-1*) is able to rescue the axon guidance defects enhanced by RNAi knockdown of *gei-17* in a *max-2*(*cy2*)-sensitized background. Mammalian *PIAS1* (*Ex Punc-25::PIAS1*) cell-autonomously rescues the defects enhanced by RNAi knockdown of *C. elegans gei-17*. RNAi knockdown of *NIL* or *col-86* served as controls. *eri-1*(*mg366*) enhances RNAi effect in neurons. (*E*) RNAi knockdown of each known gene involved in the SUMOylation pathway in *C. elegans* by soaking. Knocking-down of any of these genes significantly enhances the defects caused by *max-2* mutant. For *C*–*E*, n = 21–64. Error bars indicate SEMs. n.s., no significant difference by Student's t test; *$P < 0.05$; **$P < 0.01$; ***$P < 0.001$.

position in early embryos, DNA damage response, and development of pharyngeal muscle (30–33). However, whether GEI-17 functions in the development of the *C. elegans* nervous system has not been investigated. We showed that transgenic *gei-17* promoter GFP was expressed in the developing and adult *C. elegans* motor neurons, which started as early as the threefold stage (Fig. 2*A* and *SI Appendix*, Fig. S1*B*). In addition, mild motor axon guidance defects were observed in a *gei-17* mutant (*tm2723*) or a worm with *gei-17* RNAi knockdown (Fig. 2 *B* and *C*), indicating that *gei-17* plays a role in axon guidance.

We previously showed that *max-1* and *max-2* acted via parallel *rac*-independent and -dependent genetic pathways in UNC-5–mediated axon repulsion (34–36). Genetic interaction analysis revealed that *gei-17* did not enhance *max-1*'s axon guidance defect in *max-1;gei-17* double mutants, but *max-2's* defect was dramatically enhanced by *gei-17* in *max-2;gei-17* double mutants (Fig. 2*C*). This finding suggests *gei-17* is likely to act in the *max-1*–mediated pathway, but in parallel to the *rac*-dependent pathway involving genes like *max-2* and *ced-10* (34). Taking advantage of this result, we performed several rescue and enhancement experiments in a sensitized background using *rac* pathway mutants such as *max-2* or *ced-10* to significantly enhance the axon guidance defects of *gei-17*, which was relatively weak by itself (*SI Appendix*, Fig. S1*C*). In the sensitized *max-2* mutant background, the defects caused by *gei-17* RNAi knockdown were significantly rescued by expressing a *gei-17*/*PIAS1* cDNA specifically in motor axons under the *unc-25* promotor (Fig. 2*D*). This result indicates

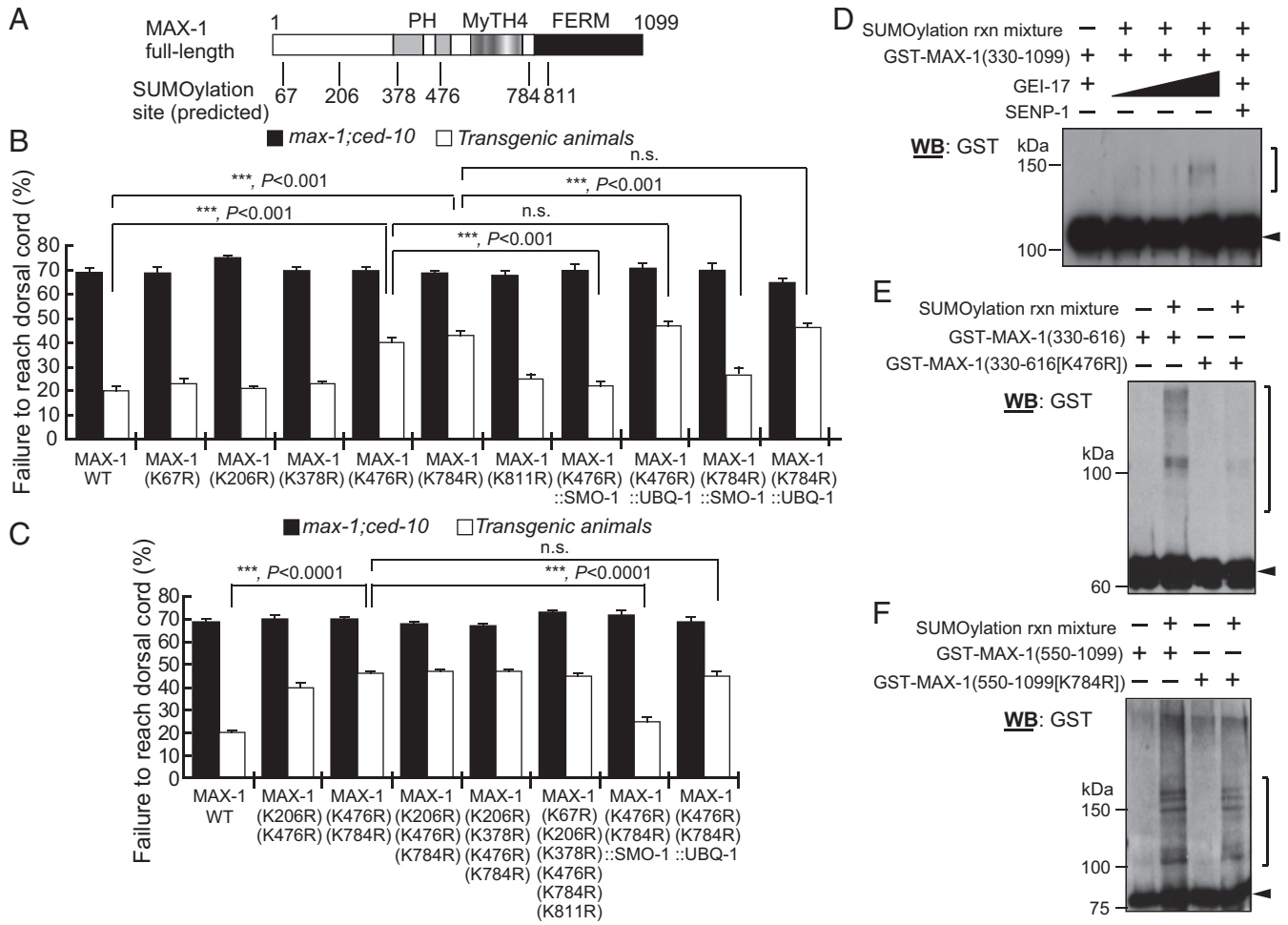

Fig. 3. SUMOylation of MAX-1 is required for its function in the guidance of motor commissural axons in *C. elegans*. (*A*) A schematic diagram of candidate SUMOylation sites of *C. elegans* MAX-1 protein predicted by SUMOplot. FERM, band 4.1/ezrin/radixin/moesin; MyTH4, myosin tail homology 4; PH, pleckstrin homology. (*B* and *C*) Quantification of the ability of MAX-1 SUMOylation site mutant variants to rescue the axon guidance defects in sensitized *max-1;ced-10* mutant background. Amino acid K-to-R mutations of the predicted SUMOylation sites were introduced into *max-1* cDNA under *unc-25* promoter. These mutant *max-1* cDNA constructs were injected into *max-1;ced-10* double-mutant worms to assess their ability to rescue the axon-guidance defects. Among all single SUMOylation site mutations, only *max-1(K476R)* and *max-1(K784R)* are unable to fully rescue the defects as WT *max-1* (*B*). The failure-to-rescue effects of *max-1(K476R)* or *max-1(K784R)* can be restored by SUMOylation mimetic *max-1(K476R)::smo-1* or *max-1(K784R)::smo-1* but not by ubiquitination mimetic *max-1(K476R)::ubq-1* or *max-1(K784R)::ubq-1* (*B*). Multiple K-to-R mutations (up to all six) of the predicted SUMOylation sites do not change the effects caused by *max-1(K476R)* or *max-1(K784R)* single mutation (*C*). The SUMOylation mimetic *max-1(K476R)(K784R)::smo-1*, but not the ubiquitination mimetic *max-1 (K476R)(K784R)::ubq-1*, can rescue the defects as does the *max-1* WT (*C*). Shown here are combined data from at least three independent generated transgenic lines. The defects were quantified and compared using transgenic animals and their nontransgenic siblings. $n = 26–56$. Error bars indicate SEMs. n.s., no significant difference by Student's *t* test; $***P < 0.001$. (*D–F*) Immunoblots of in vitro SUMOylation reactions of the recombinant proteins GST-MAX-1 (330–1099), GST-MAX-1(330–616), and GST-MAX-1(550–1099). MAX-1 is SUMOylated in vitro in a GEI-17 concentration-dependent manner (*D*). The SUMOylated GST-MAX-1(330–1099) proteins (indicated by a bracket) are not present without E1 and E2 ligase enzyme or with a SUMO-specific protease SENP-1 (*D*). K476R mutation in GST-MAX-1(330–616) attenuates SUMOylation of GST-MAX-1 fusion proteins; the bracket indicates SUMOylated GST-MAX-1(330–616) proteins (*E*). K784R mutation in GST-MAX-1(550–1099) does not attenuate SUMOylation of GST-MAX-1 fusion proteins; the bracket indicates SUMOylated GST-MAX-1(550–1099) proteins (*F*). Arrowheads in all panels indicate un-SUMOylated GST-MAX-1 fusion proteins. rxn, reaction.

that *gei-17*/*PIAS1* is involved in axon repulsion in a cell-autonomous manner.

Because GEI-17 is a SUMOylation E3 ligase, we next asked if MAX-1 was its substrate by testing whether the defects caused by *gei-17* knockdown were rescued by SUMOylated MAX-1. The function of a SUMOylated protein can be mimicked by fusing SUMO protein to its C terminus (37–39). We generated a SUMOylation mimetic *max-1* construct by fusing the *C. elegans* SUMO gene *smo-1* to *max-1* (*max-1::smo-1*). In the *max-2* mutant background, expressing the SUMOylation mimetic *max-1*, but not the WT *max-1*, significantly suppressed the axon guidance defect caused by *gei-17* RNAi knockdown (Fig. 2*D*), suggesting that SUMOylated MAX-1 can bypass the requirement for *gei-17* in axon repulsion. Accordingly, we conclude that *gei-17* acts upstream of *max-1* in axon guidance by facilitating MAX-1 SUMOylation.

SUMOylation of MAX-1 Is Required in UNC-5–Mediated Axon Repulsion. In addition to the specific substrate-recognition E3 ligases, the common components of SUMOylation pathway in *C. elegans* include the SUMO gene *smo-1*, the E1-activating enzymes *uba-2* and *aos-1*, and the E2 conjugating enzyme *ubc-9*. Using RNAi to eliminate any of these SUMOylation pathway component genes results in embryonic lethality (37, 40). To address whether the SUMOylation pathway is involved in motor axon guidance, we performed a weak RNAi knockdown

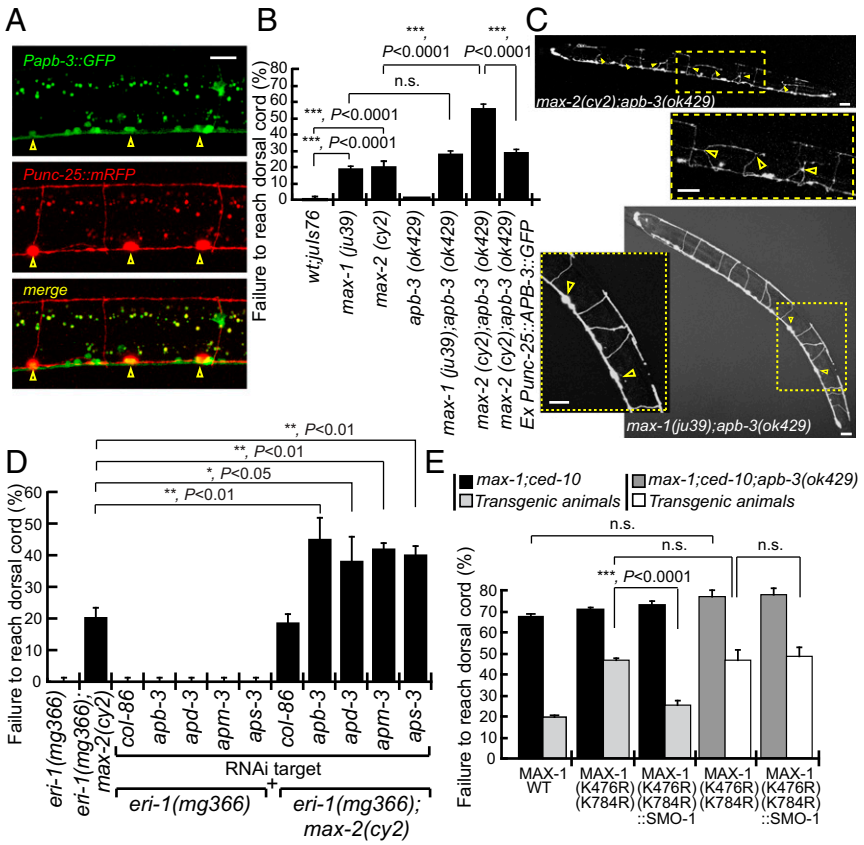

Fig. 4. The axon guidance mediated by SUMOylated MAX-1 requires *apb-3*. (*A*) *apb-3* is expressed in developing ventral cord motor neurons. At L1 stage, the *Papb-3*::GFP (green) is coexpressed with monomeric RFP driven by *unc-25* promoter (red) in DD neurons. (Scale bar: 5 μm.) Anterior is to the left and dorsal is up. (*B*) Quantification of axon guidance defects in *apb-3*, *max-1*, and *max-2* mutants. *apb-3* mutant by itself does not show axon-guidance defects, but it significantly enhances the defects of the *max-2*, but not the *max-1*, mutant. The *apb-3;max-2* defects can be cell-autonomously rescued by *Punc-25::APB-3::GFP*. (*C*) Representative images of motor commissural axon-guidance defects observed in *apb-3;max-2* (*Upper* images) and *apb-3;max-1* (*Lower* image) double mutants. Defects are indicated by arrowheads. (Scale bars: 20 μm.) (*D*) Quantification of axon-guidance defects caused by RNAi knockdown of each component of *C. elegans* AP-3 complex in the sensitized *max-2* mutant background. RNAi knockdown of each of these genes, which include genes encoding β (*apb-3*), δ (*apd-3*), μ (*apm-3*), and σ (*aps-3*) subunits, significantly enhances the defects caused by *max-2* mutant alone. *eri-1(mg366)* enhances RNAi effect in neurons; *col-86* is a control. (*E*) Quantification of genetic interactions between *apb-3* and SUMOylated MAX-1. *max-1(K476R)(K784R)* and SUMOylation mimetic *max-1(K476R)(K784R)::smo-1* were expressed in sensitized *max-1;ced-10* double-mutant background under *unc-25* promoter. The transgenic animals were then crossed into *apb-3* mutants to generate *max-1;ced-10;apb-3* triple mutants. The defects were quantified and compared using the transgenic animals and their nontransgenic siblings. For *B*, *D*, and *E*, $n = 36–64$. Error bars indicate SEMs. n.s., no significant difference by Student's *t* test; $^{*}P < 0.05$; $^{**}P < 0.01$; $^{***}P < 0.001$.

by soaking worms in diluted double-stranded RNA to avoid lethality. In the sensitized *max-2* mutant background, weak RNAi knockdown of any of the SUMOylation pathway component genes significantly enhanced the axon-guidance defect caused by *max-2* mutation alone (Fig. 2*E*). While further cell-autonomous experiments are necessary to demonstrate direct regulations of these SUMOylation pathway genes, these data together are consistent with the idea that the SUMOylation pathway is involved in motor axon guidance.

Six lysine residues in the MAX-1 protein are predicted to be SUMOylation sites (www.abgent.com/sumoplot) (Fig. 3*A*). To determine which of these lysine residues are important for its function, we generated various *max-1* cDNA mutant constructs with lysine (K) mutated to arginine (R) at these candidate sites. Each mutant's function was then evaluated in a sensitized *max-1; ced-10* double-mutant background (35). WT *max-1* rescued the axon guidance defect of the *max-1;ced-10* double mutant by reducing the 70% failure rate to 20%. Among the six *max-1* constructs with a single K-to-R mutation, only *max-1(K476R)* or *max-1(K784R)* was unable to significantly rescue the defects, compared with WT or other mutants (Fig. 3*B*). However, the SUMOylation mimetic *max-1(K476R)::smo-1* or *max-1(K784R)::smo-1* regained the ability to rescue the defects as the WT *max-1* did, indicating that K476R or K784R is essential for MAX-1 SUMOylation (Fig. 3*B*). As a control, the *max-1(K476R)* or *max-1(K784R)* fused with the *C. elegans* ubiquitin gene *ubq-1* did not have the same effects (Fig. 3*B*). Interestingly, multiple point mutation constructs from double up to sextuple did not further change the effects observed in either K476R or K784R alone (Fig. 3*C*). These results together indicate that K476 and K784 are required for MAX-1–mediated axon guidance, and that these two sites are in the same SUMOylation genetic pathway.

An in vitro SUMOylation assay on GST-fused MAX-1 peptide [amino acid residue 330–1099; labeled as GST-MAX-1(330–1099)] confirmed that MAX-1 was SUMOylated in the presence of GEI-17 in a concentration-dependent manner and this SUMOylation effect was eliminated by adding the SUMO-specific protease SENP-1 (Fig. 3*D*). When GST-MAX-1(330–1099) was further split into two peptides—GST-MAX-1(330–616), which contains K476, and GST-MAX-1(550–1099), which contains K784—both could be SUMOylated in vitro (Fig. 3 *E* and *F*). However, when the MAX-1 peptide with either K476R or K784R mutation was tested, SUMOylated MAX-1(K476R) peptide was undetectable (Fig. 3*E*), but SUMOylated MAX-1

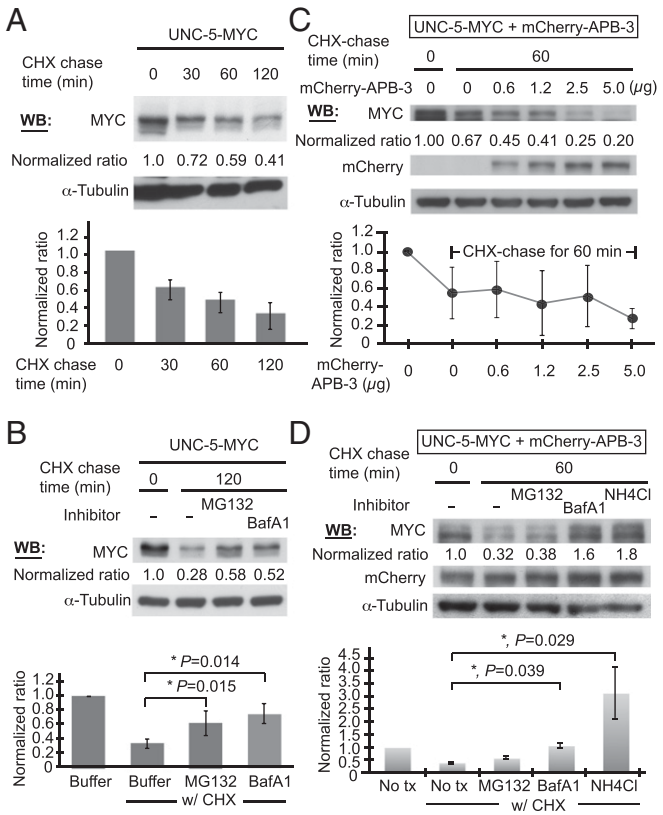

Fig. 5. Overexpression of APB-3 regulates UNC-5 degradation. (*A*) CHX (50 μg/mL) chase of UNC-5-MYC proteins transiently expressed in COS cells. Immunoblotting was performed with anti-MYC antibody to detect the amount of UNC-5-MYC proteins and with anti–α-tubulin antibody to normalize the loading amount. Bar graphs show the normalized ratio of UNC-5-MYC proteins in each lane with the SD derived from seven replicate experiments. (*B*) UNC-5-MYC–transfected COS cells were treated with CHX for 2 h in the presence of MG132 (10 μM) or BafA1 (10 nM). Bar graphs show the normalized ratio of UNC-5-MYC proteins from triplicate experiments. The *P* values were estimated by one-way ANOVA with Holm–Sidak post hoc comparison. Both MG132 and BafA1 treatments partially inhibit UNC-5 degradation. (*C*) Representative immunoblots of protein lysates of COS cells cotransfected with UNC-5-MYC and various amounts of mCherry-APB-3 after 1 h CHX chase. The line graph shows results of seven replicates with the dots representing the average value. Error bars indicated SDs. Overexpression of APB-3 enhances the degradation of UNC-5 in a concentration-dependent manner. (*D*) Representative immunoblots of protein lysates of COS cells cotransfected with UNC-5-MYC and mCherry-APB-3 with or without MG132, BafA1, or NH_4Cl (2 M) treatment after 1 h CHX chase. The *P* values in bar graph were estimated by Mann-Whitney rank sum test based on four independent experiments. Error bars indicate SEMs. The lysosome acidifier blockers, BafA1 and NH_4Cl, inhibit UNC-5 degradation. By contrast, the proteasome inhibitor MG132 does not inhibit UNC-5 degradation in the presence of APB-3. Normalized ratios in all panels were calculated by comparing the intensities of each band estimated via ImageJ to the intensity of the sample before chasing (left-most lane) after normalization to the intensity of each respective α-tubulin band as a loading control. $*P < 0.05$. BafA1, bafilomycin A1; CHX, cycloheximide; tx, treatment.

(K784R) peptide was still present (Fig. 3*F*), suggesting that K476 amino acid is the primary SUMO acceptor site of MAX-1 protein. Taken together, these data suggest that GEI-17 can SUMOylate MAX-1 at specific lysine sites and such GEI-17–mediated SUMOylation of MAX-1 is required for the function of MAX-1 in regulating dorsal guidance of motor axons.

***apb-3* Functions Downstream of *max-1* to Regulate *unc-5*–Mediated Axon Repulsion.** We found that *apb-3* was also expressed in *C. elegans* motor neurons (Fig. 4*A*). Although the *apb-3(ok429)* mutant did not exhibit an obvious axon guidance defect, it significantly enhanced the defect in *max-2* but not in *max-1* mutants (Fig. 4 *B* and *C*), suggesting that *apb-3*, like *gei-17*, functions in the *max-1*–mediated signaling pathway. This *max-2* phenotype enhancement caused by *apb-3* mutant was rescued by the expression of a WT *apb-3* cDNA driven by the motor neuron-specific *unc-25* promoter (Fig. 4*B*). Thus, *apb-3* is cell-autonomously involved in the *max-1*–mediated signaling pathway in motor neurons. AP-3 is a heterotetrameric complex composed of β, δ, μ, and σ subunits (27). In addition to *apb-3* (the β subunit gene), RNAi knockdown of δ subunit gene *apd-3*, μ subunit gene *apm-3*, or σ subunit *aps-3* similarly enhanced the defect of *max-2* mutant, suggesting that AP-3 complex is involved in the motor axon guidance (Fig. 4*D*).

To determine the genetic epistasis between *apb-3* and *max-1*, we crossed *apb-3(ok429)* into *max-1;ced-10* double mutants expressing either MAX-1 SUMOylation mutant MAX-1(K476R)(K784R) or SUMOylation-mimetic MAX-1(K476R)(K784R)::SMO-1 (Fig. 4*E*). As shown earlier (Fig. 3*C*), MAX-1(K476R)(K784R) could only partially rescue the defects in the *max-1;ced-10* double mutants, but the SUMOylation-mimetic MAX-1(K476R)(K784R)::SMO-1 significantly suppressed the defects, producing a similar phenotype to WT MAX-1. By contrast, in the *apb-3;max-1;ced-10* triple mutant, the SUMOylation-mimetic MAX-1(K476R)(K784R)::SMO-1 was unable to further suppress the defects compared with MAX-1(K476R)(K784R), indicating that *apb-3* is required for SUMOylated MAX-1 to function properly. This effect was not due to the pleiotropic effect of *apb-3*, since *apb-3* mutation did not enhance the defect of *max-1;ced-10* double mutant and transgenic animals expressing MAX-1(K476R)(K784R) showed similar axon guidance defect with or without *apb-3* mutation (Fig. 4*E*). Collectively, these data demonstrate that the APB-3–containing AP-3 complex acts downstream of SUMOylated MAX-1 to regulate motor axon repulsion.

The UNC-5 Receptor Is Routed to Lysosomes by Overexpressing APB-3. In cultured cortical neurons, UNC-5 was partially colocalized with a trans-Golgi marker (TGN p230) and lysosome-associated membrane protein 1 (LAMP-1). The AP-3 complex has previously been shown to reside in these organelles for cargo sorting and degradation (*SI Appendix*, Fig. S2 *A* and *B*) (22, 27), suggesting that UNC-5 might be degraded in the lysosome via AP-3 complex. To explore this possibility, we turned to COS cells where no endogenous MAX-1 or UNC-5 is expressed. The half-life of the turnover of UNC-5 overexpressed in COS cells was ∼60 min, as determined by a cycloheximide-chase experiment (Fig. 5*A*). Either the proteasome inhibitor MG132 or the lysosome acidifier blocker bafilomycin A1 partially inhibited the degradation of UNC-5, suggesting that both the ubiquitin-proteasome system and the lysosomal degradation pathway are involved in the degradation of UNC-5 (Fig. 5*B*). Intriguingly, when UNC-5 was coexpressed with APB-3 in COS cells, UNC-5 degradation was accelerated. This effect depended on APB-3 concentration, with UNC-5 degradation seeming to saturate at higher APB-3 concentrations (Fig. 5*C*). In addition, when UNC-5 was coexpressed with APB-3, MG132 treatment no longer protected UNC-5 from degradation. By contrast, lysosome blockers, either BafA1 or NH_4Cl, still inhibited UNC-5 degradation (Fig. 5*D*). These data suggest that UNC-5 is preferentially routed to the lysosomal degradation pathway in the presence of APB-3.

Interaction Between UNC-5 and MAX-1 Is Modulated by MAX-1 SUMOylation and APB-3. SUMOylation modifies protein's surface structure and can change its ability to interact with other proteins (41). We previously reported that MAX-1 did not seem to interact with UNC-5 (10). However, by adjusting the coimmunoprecipitation condition, we were able to demonstrate that MAX-1 did interact with UNC-5, as they reciprocally coprecipitated each other in a protein complex (Fig. 6*A*). The previous negative

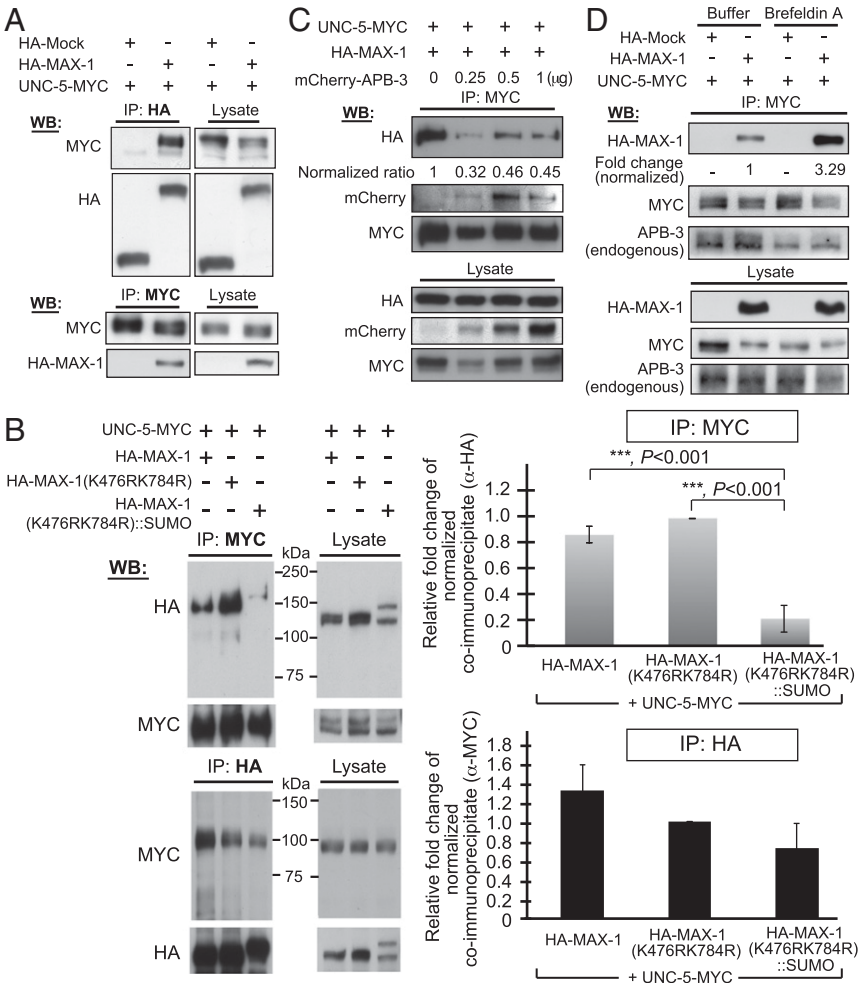

Fig. 6. Biochemical interaction of MAX-1 and UNC-5 is modulated by MAX-1 SUMOylation and APB-3. (*A*) Immunoblots of lysates of cotransfected COS cells show reciprocal coimmunoprecipitation of UNC-5 and MAX-1. (*B*) Representative immunoblots show the amount of SUMOylation mimetic MAX-1 in the UNC-5 immunoprecipitate is significantly reduced (*Upper*). Likewise, less UNC-5 is immunoprecipitated by SUMOylation mimetic MAX-1 (*Lower*). For quantification, the amount of each coimmunoprecipitate was normalized by the amount of the tagged protein immunoprecipitated by the indicated antibody. The normalized amount was then adjusted to the input and compared with that of the MAX-1 SUMOylation mutant MAX-1(K476R)(K784R) to quantify the relative fold change. The *P* values shown in the bar graph were estimated by one-way ANOVA with Holm–Sidak post hoc comparison from more than triplicate experiments. Error bars indicate SDs. ***$P < 0.001$. (*C*) Immunoblots show that overexpression of APB-3 reduces the amount of MAX-1 proteins in UNC-5 immunoprecipitates. Note that a relatively low amount of APB-3 overexpression is sufficient to achieve its maximal interference effect with the presence of APB-3 in the UNC-5 immunoprecipitates. (*D*) Immunoblots show that Brefeldin A treatment (2 μg/mL) increases the amount of MAX-1 protein in UNC-5 immunoprecipitates. Note that Brefeldin A treatment decreases the amount of endogenous APB-3 included in the immunoprecipitates.

result might have occurred because overexpressed MAX-1 is modified by SUMOylation in COS cells, so that the interaction was too unstable to detect. We tested this hypothesis by using SUMOylation-mimetic MAX-1 and found that SUMOylated MAX-1 significantly lost its binding affinity to UNC-5 (Fig. 6*B*).

Domain mapping analysis revealed that the ZU5 domain of UNC-5, which is responsible for its interaction with APB-3 (Fig. 1*H*), also interacted with MAX-1 (*SI Appendix*, Fig. S3*A*), suggesting that APB-3 might compete with MAX-1 for interaction with UNC-5. Indeed, overexpressing APB-3 significantly interfered with the binding of MAX-1 to UNC-5 (Fig. 6*C*). APB-3 seemed to have higher affinity for UNC-5 than did MAX-1, as a small amount of APB-3 expression is sufficient to achieve maximal interference with UNC-5's binding to MAX-1 (Fig. 6*C*). We further demonstrated that using Brefeldin A to deplete the insertion of AP-3 complex into intracellular vesicular membrane increased colocalization of MAX-1 with UNC-5 in the cytoplasmic vesicles of transfected COS cells (*SI Appendix*, Fig. S3*B*) and enhanced protein complex formation between MAX-1 and UNC-5 despite the presence of APB-3 (Fig. 6*D*). This result suggests that the AP-3 complex on the intracytoplasmic vesicles can specifically interfere with binding between MAX-1 and UNC-5. Together, these results indicate that the interaction between UNC-5 and MAX-1 is modulated by MAX-1 SUMOylation and by the level of AP-3 complex in the intracellular vesicles.

Genetic interaction analysis indicates *max-1* is upstream of *apb-3* in regulating *unc-5*–mediated axon repulsion, which raises the possibility that MAX-1 might mediate UNC-5 degradation through APB-3. We found that MAX-1 and APB-3 did not interact with each other biochemically (*SI Appendix*, Fig. S3*D*). MAX-1 alone was degraded mainly through the endolysosomal pathway, given that the lysosome blocker NH_4Cl but not the proteasome inhibitor MG132 prevented MAX-1 from degradation (*SI Appendix*, Fig. S3*C*). In addition, the turnover time of UNC-5 was not affected by overexpressing MAX-1, SUMOylation mutant MAX-1(K476R)(K784R), or SUMOylation-mimetic MAX-1 (*SI Appendix*, Fig. S2*C*). Likewise, the degradation of MAX-1 was not affected by coexpressed UNC-5 either (*SI*

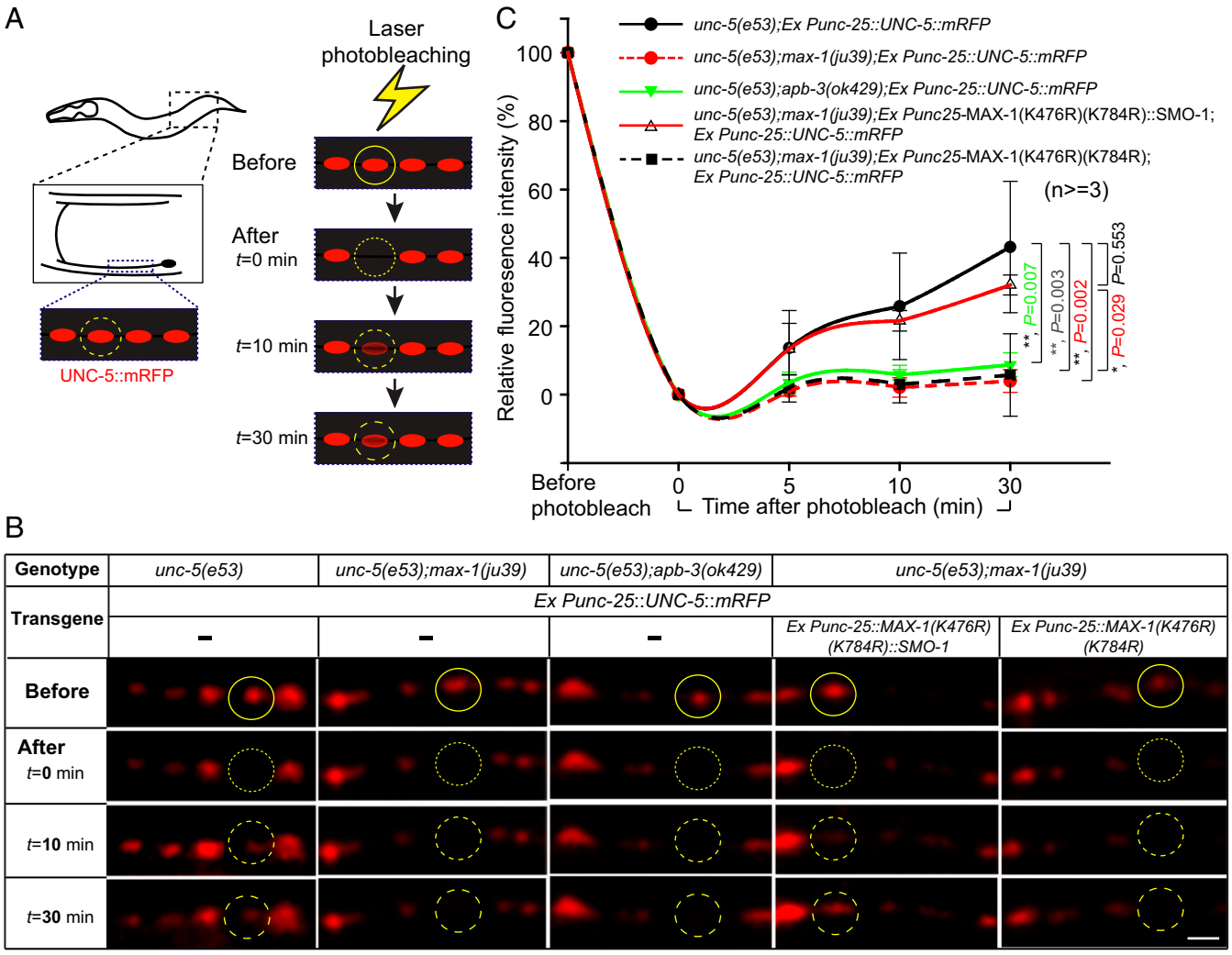

Fig. 7. Regulation of UNC-5 receptor trafficking in *C. elegans* axons in vivo requires APB-3 and SUMOylated MAX-1. (*A*) Schematic diagrams to show the punctated (red dots) expression pattern of UNC-5::mRFP in a *C. elegans* motor axon (*Left*) and the FRAP experimental procedures (*Right*). The approximate axon segment shown in images in *B* is indicated in the boxed area. (*B*) Representative FRAP time-course images showing that the recoveries of UNC-5::mRFP puncta after photobleaching (oval areas) are impaired in *max-1* and *apb-3* mutant backgrounds. The impaired recoveries of UNC-5::mRFP puncta in the *max-1* mutant background are cell-autonomously rescued by SUMOylation mimetic *max-1* [*MAX-1(K476R)(K784R)::SMO-1*], but not by SUMOylation-mutated *max-1* [*MAX-1(K476R)(K784R)*]. (Scale bar: 5 μm.) (*C*) The average FRAP recovery profiles from each set of experiments are shown as scattered line plots. The *P* values shown at $t = 30$ min were calculated by one-way ANOVA with Holm–Sidak post hoc comparison. $n \geq 3$. Error bars indicate SDs. $^*P < 0.05$; $^{**}P < 0.01$.

Appendix, Fig. S3*E*). These results suggest that, while UNC-5 forms a protein complex with MAX-1, the degradation of UNC-5 and MAX-1 in lysosomes is independently regulated.

Both SUMOylated MAX-1 and APB-3 Regulate UNC-5 Trafficking Along the Axons. The AP-3 complex is involved not only in regulating protein degradation but also in sorting and trafficking intracellular vesicles (22, 23, 28, 42). To address how MAX-1 and APB-3 regulate the trafficking of vesicles carrying UNC-5 receptor, we generated a transgenic line expressing monomeric RFP-tagged UNC-5 (UNC-5::mRFP) in *C. elegans* motor axons. As shown previously (8), UNC-5::mRFP accumulated as puncta along the motor axons (Fig. 7*A*). In *max-1* or *apb-3* mutants, punctated UNC-5::mRFP was still observed, indicating that UNC-5 receptors were transported along axons in these mutants. We then performed fluorescence recovery after photobleaching (FRAP) experiments to access the dynamics of UNC-5 receptor trafficking along axons. In *unc-5* mutants that were rescued by specifically expressing UNC-5::mRFP in motor neurons (producing WT motor axons), 43% recovery of fluorescent intensity was observed at 30 min after photobleaching (Fig. 7 *B* and *C*). However, when these transgenic worms were in the *max-1* mutant background, the recovery was significantly reduced to 4%. Similarly, in the transgenics under *apb-3* mutant background, only 9% recovery was observed (Fig. 7 *B* and *C*). Therefore, both *max-1* and *apb-3* are involved in regulating the dynamics of UNC-5 transportation along the axon in vivo.

We next performed FRAP in these transgenics under *max-1* mutant background but expressing either *max-1(K476R)(K784R)* or *max-1(K476R)(K784R)::smo-1*. As shown in Fig. 7 *B* and *C*, *max-1(K476R)(K784R)::smo-1* rescued the recovery rate of fluorescent intensity significantly better than *max-1(K476R)(K784R)* (32% vs. 6%; $P = 0.029$). Altogether, these data indicate that the trafficking of UNC-5 receptor in the axon is regulated by both SUMOylated MAX-1 and APB-3.

Discussion

SUMOylation of MAX-1 Regulates UNC-5–Mediated Axon Repulsion. In this study, we identified the SUMOylation E3 ligase GEI-17/PIAS1 as a regulator of MAX-1 and demonstrated that MAX-1

SUMOylation is critical for UNC-5–mediated axon repulsion. Detailed molecular, genetic, and biochemical analysis revealed that MAX-1 acts as a dynamic regulator of the UNC-5 receptor: MAX-1 constitutively binds to UNC-5 receptor in axons but dissociates from UNC-5 when MAX-1 is SUMOylated. This dynamic switch regulates the trafficking and degradation of UNC-5 receptor.

Our results show that SUMOylation of the conserved K476 amino acid in MAX-1 is essential for its function. Another amino acid, K784, is also required for MAX-1's function genetically, but biochemical evidence suggests it is not a primary SUMO acceptor site. Because SUMOylation-mimetic *MAX-1(K784R)::smo-1* rescues the axon-guidance defect caused by *max-1* mutation, K784 might have a modulatory role in MAX-1's function. Posttranslational modifications such as phosphorylation, ubiquitination, and acetylation can modify a potential SUMO acceptor site to change its SUMOylation status (13, 14). Such intramolecular "cross-talk" between posttranslational modifications has been reported for several SUMOylated proteins (13, 43, 44). It will therefore be interesting to know how the SUMO acceptor sites of MAX-1 are regulated by other posttranslational modifications.

Another important question to be addressed is how the SUMOylation E3 ligase GEI-17 is activated. Our current data do not provide information on the activation of GEI-17, although we know that both the *gei-17* gene and SUMOylation of MAX-1 are required for normal function of UNC-5. It remains to be investigated whether the signaling of the UNC-5 receptor activated by UNC-6 triggers the activation of GEI-17 and the subsequent SUMOylation of MAX-1.

AP-3 Routes UNC-5 Degradation Through the Lysosomal Pathway and Modulates UNC5 Trafficking Along the Axon. The AP-3 complex is one of the intracellular coat protein complexes that function as adaptors for vesicular sorting (23, 27, 29). We found that AP-3 complex directs the UNC-5 receptor to the lysosomal pathway for accelerated turnover. In cultured mammalian neurons, UNC-5 receptors are internalized by endocytosis upon stimulation of UNC-6 (6). We therefore envision that an increase in UNC-5–containing vesicles sorted by AP-3 for degradation in lysosomes can provide a mechanism for shutting down the UNC-5 signaling activated by UNC-6 during axon guidance.

Our in vivo FRAP study suggests that the AP-3 complex is involved in regulating the trafficking of UNC-5 receptor in axons, which also requires SUMOylated MAX-1. However, this approach does not address the nature of UNC-5–associated vesicles and the directionality of UNC-5 transportation along the axon. Neither does it address whether the control of such trafficking is related to UNC-5 degradation. Nevertheless, given our genetic data showing *apb-3* is required for *max-1* to regulate UNC-5–mediated axon repulsion, we suspect that AP-3 acts via degradation and protein trafficking, as well as its coordination with MAX-1, in the dynamic control of UNC-5 receptors during axon guidance.

The regulation of UNC-5 receptor by AP-3 complex is likely to involve other molecular mechanisms. AP-3, like other AP adaptor complexes, recognizes a conserved sorting motif, the dileucine motif (D/E)XXXL(L/I), on vesicle cargo proteins and facilitates the assembly and sorting of vesicles by binding the vesicular trafficking machinery, such as BLOC-1 and HOPS (27). Phosphorylated (S/T)XXXL(L/I) mimics the dileucine sorting motif (D/E)XXXL(L/I) for binding adaptor protein complexes (45–48). An (S/T)XXXL(L/I) motif can be identified in the ZU5 domain of UNC-5 (amino acid 520–525). We demonstrate here that the ZU5 domain binds APB-3 directly and that mutations of the amino acids L(524)I(525) to A(524)A(525) disrupt the interaction between UNC-5 and APB-3 (Fig. 1*G*). Thus, we reason that, after phosphorylation, the (S/T)XXXL(L/I) motif on the ZU5 domain of UNC-5 can function as an AP-3 binding dileucine motif. As several protein kinases or phosphatases are involved in UNC-5–mediated axon guidance (8, 9, 35, 49, 50), it is likely that the interaction of AP-3 with UNC-5 is activated by regulated phosphorylation.

A Model for SUMOylated MAX-1 and AP-3 in the Regulation of UNC-5 Receptors During Axon Repulsion. Previous studies have clearly demonstrated that the ZU5 domain of UNC-5 receptor is crucial for axon guidance (51–53). Here we show that MAX-1 and APB-3 competitively bind the ZU5 domain of UNC-5 and together they regulate the guidance of *C. elegans* motor axons. Genetically, *max-1* acts upstream of *apb-3* in the *unc-5*–mediated axon repulsion. Both *max-1* and *apb-3* are required for UNC-5 receptor trafficking in axons. In addition, our biochemical analysis indicates that APB-3 has stronger binding affinity to UNC-5 than does MAX-1 and that SUMOylated MAX-1 weakens its binding with UNC-5. Although APB-3 facilitates UNC-5 degradation, MAX-1, with or without SUMOylation, does not affect the degradation of UNC-5 regulated by APB-3.

We therefore propose the following model (*SI Appendix*, Fig. S4): MAX-1 is a dynamic regulator of UNC-5 receptor in the axon. MAX-1 constitutively binds to UNC-5 receptor during axonal development. When the SUMOylation E3 ligase PIAS1/GEI-17 is activated, either through ligand binding to UNC-5 receptor or via other unidentified mechanisms, MAX-1 is SUMOylated. As a consequence, UNC-5 receptor is dissociated from SUMOylated MAX-1, favoring more interaction between UNC-5 receptor and other molecules such as APB-3. Thus, MAX-1 acts as a modulatory molecular switch to regulate UNC-5 receptor's intracellular interactions. In the presence of AP-3 complex, after dissociating from SUMOylated MAX-1, UNC-5 receptor can be sorted for trafficking in the axon and/or routed for endolysosomal degradation. Without MAX-1, as in the *max-1* mutant, the trafficking and degradation of UNC-5 receptors are dysregulated, resulting in axon-guidance defects. Overexpressing *unc-5*, which presumably provides more available surface UNC-5 receptors, can thus partially rescue the axon guidance defects in *max-1* mutants (10).

Guiding axons through concentration gradients of environmental cues is an essential mechanism for forming a proper neuronal connection network. During axon repulsion, the growing axons migrate by sensing concentration differences of the guidance cues. Because the concentration differences along the gradient are constantly changing, the navigating growth cone has to actively regulate its response so that it can move directly away from the guidance cue (54, 55). Previous studies have demonstrated regulated interactions of ligands (UNC-6 and UNC-129) and receptors (UNC-5 and UNC-40) are essential for dorsal repulsion of motor axons. The growth cone is initially repelled by a high concentration of UNC-6 through UNC-5 receptor alone, but when the growth cone moves dorsally and the concentration of UNC-6 in the environment becomes low, the UNC-5 receptor needs both UNC-129 and UNC-40 to properly guide the axons (5). However, these studies did not address an alternative mechanism by which the UNC-5 receptor itself is regulated (56).

Lysosomal degradation of proteins can occur in the growth cone locally (57). If UNC-6 binding to UNC-5 could trigger PIAS1/GEI-17 activation, our model (*SI Appendix*, Fig. S4) could provide a potential alternative for how UNC-5 receptor is regulated locally when the growth cone is moving away from the UNC-6 gradient. Regulated degradation of surface receptors in response to a morphogen concentration gradient would lead to a dampened response downstream of the receptors in the high-concentration morphogen field but a heightened response in the low-concentration field (58). Consistent with this effect, our model (*SI Appendix*, Fig. S4) predicts that the surface availability of UNC-5 is increased at low UNC-6 concentration due to less activation of PIAS1/GEI-17 and thus less UNC-5 degradation. In addition, in a model predicting the variability and the reliability of biological response toward a diffusible morphogen concentration gradient (59), changes in available receptors would result

in a shift in amount of surface receptor occupancy, which reduces the accuracy of the response where the ligand concentration is low. Based on our findings that MAX-1 and AP-3 regulate the trafficking and degradation of UNC-5 receptor, we can predict that the guidance of axon is most likely to be affected where the concentration of UNC-6 is low. Consistent with this prediction, misguided DA and DB motor axons turn prematurely only in the dorsal half of *max-1* mutants, where UNC-6 is low (10).

Materials and Methods

Details are provided in *SI Appendix, SI Materials and Methods*, including detailed methods for yeast two-hybrid screen, *C. elegans* RNAi experiments, *C. elegans* phenotypic analysis, FRAP experiments, in vitro SUMOylation assay, in vitro binding assay, cell culture and transfection, fluorescence microscope, immunoblotting, pulse-chase experiments, coimmunoprecipitation, and statistical analysis. The information about *C. elegans* strains and the generation of plasmids and transgene constructs are also described in *SI Appendix, SI Materials and Methods*.

ACKNOWLEDGMENTS. We thank the International *C. elegans* Gene Knockout Consortium for strains. We are grateful to Yuji Kohara, Ken-Ichi Ogura, Yoshio Goshima, Gary Ruvkun, Andy Fire, and Lindsay Hinck for materials. We thank Li-Ting Jang and Fang-Jen Lee for their contributions in the initial stage of *apb-3* studies, and Chun-Chen Ho for the in vitro SUMOylation assays. We also thank Abraham Noorbakhsh, Kimberly Zhou, and Chin-Min Ho for technical help and Noelle L'Etoile, Ting-Wen Cheng, Damien O'Halloran, Scott Hamilton, Bi-Tzeng Juang, the members of the H.-J.C. and P.-H.H. labs, and the members of the University of California, Davis (UC Davis) "Super Worm Group" for comments and advise. This work was supported in part by a Health System grant from UC Davis (to H.-J.C.) and a grant from National Taiwan University College of Medicine (to P.-H.H.).

1. Kolodkin AL, Tessier-Lavigne M (2011) Mechanisms and molecules of neuronal wiring: A primer. *Cold Spring Harb Perspect Biol* 3:a001727.
2. O'Donnell M, Chance RK, Bashaw GJ (2009) Axon growth and guidance: Receptor regulation and signal transduction. *Annu Rev Neurosci* 32:383–412.
3. Araújo SJ, Tear G (2003) Axon guidance mechanisms and molecules: Lessons from invertebrates. *Nat Rev Neurosci* 4:910–922.
4. Wadsworth WG (2002) Moving around in a worm: Netrin UNC-6 and circumferential axon guidance in C. elegans. *Trends Neurosci* 25:423–429.
5. MacNeil LT, Hardy WR, Pawson T, Wrana JL, Culotti JG (2009) UNC-129 regulates the balance between UNC-40 dependent and independent UNC-5 signaling pathways. *Nat Neurosci* 12:150–155.
6. Bartoe JL, et al. (2006) Protein interacting with C-kinase 1/protein kinase Calpha-mediated endocytosis converts netrin-1-mediated repulsion to attraction. *J Neurosci* 26:3192–3205.
7. Moore SW, Kennedy TE (2006) Protein kinase A regulates the sensitivity of spinal commissural axon turning to netrin-1 but does not switch between chemoattraction and chemorepulsion. *J Neurosci* 26:2419–2423.
8. Ogura K, Goshima Y (2006) The autophagy-related kinase UNC-51 and its binding partner UNC-14 regulate the subcellular localization of the netrin receptor UNC-5 in Caenorhabditis elegans. *Development* 133:3441–3450.
9. Williams ME, Wu SC, McKenna WL, Hinck L (2003) Surface expression of the netrin receptor UNC5H1 is regulated through a protein kinase C-interacting protein/protein kinase-dependent mechanism. *J Neurosci* 23:11279–11288.
10. Huang X, Cheng HJ, Tessier-Lavigne M, Jin Y (2002) MAX-1, a novel PH/MyTH4/FERM domain cytoplasmic protein implicated in netrin-mediated axon repulsion. *Neuron* 34:563–576.
11. Zhong H, et al. (2006) Vertebrate MAX-1 is required for vascular patterning in zebrafish. *Proc Natl Acad Sci USA* 103:16800–16805.
12. Rytinki MM, Kaikkonen S, Pehkonen P, Jääskeläinen T, Palvimo JJ (2009) PIAS proteins: Pleiotropic interactors associated with SUMO. *Cell Mol Life Sci* 66:3029–3041.
13. Gareau JR, Lima CD (2010) The SUMO pathway: Emerging mechanisms that shape specificity, conjugation and recognition. *Nat Rev Mol Cell Biol* 11:861–871.
14. Geiss-Friedlander R, Melchior F (2007) Concepts in sumoylation: A decade on. *Nat Rev Mol Cell Biol* 8:947–956.
15. Johnson ES (2004) Protein modification by SUMO. *Annu Rev Biochem* 73:355–382.
16. Berdnik D, Favaloro V, Luo L (2012) The SUMO protease Verloren regulates dendrite and axon targeting in olfactory projection neurons. *J Neurosci* 32:8331–8340.
17. Craig TJ, Henley JM (2012) Protein SUMOylation in spine structure and function. *Curr Opin Neurobiol* 22:480–487.
18. Guo C, et al. (2013) SENP3-mediated deSUMOylation of dynamin-related protein 1 promotes cell death following ischaemia. *EMBO J* 32:1514–1528.
19. Henley JM, Craig TJ, Wilkinson KA (2014) Neuronal SUMOylation: Mechanisms, physiology, and roles in neuronal dysfunction. *Physiol Rev* 94:1249–1285.
20. Krumova P, et al. (2011) Sumoylation inhibits alpha-synuclein aggregation and toxicity. *J Cell Biol* 194:49–60.
21. Mojsa B, Mora S, Bossowski JP, Lassot I, Desagher S (2015) Control of neuronal apoptosis by reciprocal regulation of NFATc3 and Trim17. *Cell Death Differ* 22:274–286.
22. Dell'Angelica EC (2009) AP-3-dependent trafficking and disease: The first decade. *Curr Opin Cell Biol* 21:552–559.
23. Park SY, Guo X (2014) Adaptor protein complexes and intracellular transport. *Biosci Rep* 34:e00123.
24. Faúndez V, Horng JT, Kelly RB (1998) A function for the AP3 coat complex in synaptic vesicle formation from endosomes. *Cell* 93:423–432.
25. Salem N, Faúndez V, Horng J-T, Kelly RB (1998) A v-SNARE participates in synaptic vesicle formation mediated by the AP3 adaptor complex. *Nat Neurosci* 1:551–556.
26. Danglot L, Galli T (2007) What is the function of neuronal AP-3? *Biol Cell* 99:349–361.
27. Newell-Litwa K, Seong E, Burmeister M, Faundez V (2007) Neuronal and non-neuronal functions of the AP-3 sorting machinery. *J Cell Sci* 120:531–541.
28. Li P, Merrill SA, Jorgensen EM, Shen K (2016) Two clathrin adaptor protein complexes instruct axon-dendrite polarity. *Neuron* 90:564–580.
29. Gomez-Navarro N, Miller EA (2016) COP-coated vesicles. *Curr Biol* 26:R54–R57.
30. Ferreira HC, Towbin BD, Jegou T, Gasser SM (2013) The shelterin protein POT-1 anchors Caenorhabditis elegans telomeres through SUN-1 at the nuclear periphery. *J Cell Biol* 203:727–735.
31. Kim SH, Michael WM (2008) Regulated proteolysis of DNA polymerase eta during the DNA-damage response in C. elegans. *Mol Cell* 32:757–766.
32. Pelisch F, et al. (2017) A SUMO-dependent protein network regulates chromosome congression during oocyte meiosis. *Mol Cell* 65:66–77.
33. Roy Chowdhuri S, Crum T, Woollard A, Aslam S, Okkema PG (2006) The T-box factor TBX-2 and the SUMO conjugating enzyme UBC-9 are required for ABa-derived pharyngeal muscle in C. elegans. *Dev Biol* 295:664–677.
34. Chen SY, Huang PH, Cheng HJ (2011) Disrupted-in-Schizophrenia 1-mediated axon guidance involves TRIO-RAC-PAK small GTPase pathway signaling. *Proc Natl Acad Sci USA* 108:5861–5866.
35. Lucanic M, Kiley M, Ashcroft N, L'etoile N, Cheng H-J (2006) The Caenorhabditis elegans P21-activated kinases are differentially required for UNC-6/netrin-mediated commissural motor axon guidance. *Development* 133:4549–4559.
36. Lucanic M, Cheng HJ (2008) A RAC/CDC-42-independent GIT/PIX/PAK signaling pathway mediates cell migration in C. elegans. *PLoS Genet* 4:e1000269.
37. Leight ER, Glossip D, Kornfeld K (2005) Sumoylation of LIN-1 promotes transcriptional repression and inhibition of vulval cell fates. *Development* 132:1047–1056.
38. Ross S, Best JL, Zon LI, Gill G (2002) SUMO-1 modification represses Sp3 transcriptional activation and modulates its subnuclear localization. *Mol Cell* 10:831–842.
39. Shalizi A, et al. (2006) A calcium-regulated MEF2 sumoylation switch controls postsynaptic differentiation. *Science* 311:1012–1017.
40. Zhang H, et al. (2004) SUMO modification is required for in vivo Hox gene regulation by the Caenorhabditis elegans Polycomb group protein SOP-2. *Nat Genet* 36:507–511.
41. Cox E, et al. (2017) Global analysis of SUMO-binding proteins identifies SUMOylation as a key regulator of the INO80 chromatin remodeling complex. *Mol Cell Proteomics* 16:812–823.
42. Asensio CS, Sirkis DW, Edwards RH (2010) RNAi screen identifies a role for adaptor protein AP-3 in sorting to the regulated secretory pathway. *J Cell Biol* 191:1173–1187.
43. Bergink S, Jentsch S (2009) Principles of ubiquitin and SUMO modifications in DNA repair. *Nature* 458:461–467.
44. Ulrich HD (2014) Two-way communications between ubiquitin-like modifiers and DNA. *Nat Struct Mol Biol* 21:317–324.
45. Dietrich J, Hou X, Wegener AM, Geisler C (1994) CD3 gamma contains a phosphoserine-dependent di-leucine motif involved in down-regulation of the T cell receptor. *EMBO J* 13:2156–2166.
46. Gibson RM, et al. (2000) Phosphorylation of human gp130 at Ser-782 adjacent to the di-leucine internalization motif: Effects on expression and signaling. *J Biol Chem* 275:22574–22582.
47. Pitcher C, Höning S, Fingerhut A, Bowers K, Marsh M (1999) Cluster of differentiation antigen 4 (CD4) endocytosis and adaptor complex binding require activation of the CD4 endocytosis signal by serine phosphorylation. *Mol Biol Cell* 10:677–691.
48. von Essen M, et al. (2002) The CD3 gamma leucine-based receptor-sorting motif is required for efficient ligand-mediated TCR down-regulation. *J Immunol* 168:4519–4523.
49. Han J, Han L, Tiwari P, Wen Z, Zheng JQ (2007) Spatial targeting of type II protein kinase A to filopodia mediates the regulation of growth cone guidance by cAMP. *J Cell Biol* 176:101–111.
50. Ogura K, et al. (2010) Protein phosphatase 2A cooperates with the autophagy-related kinase UNC-51 to regulate axon guidance in Caenorhabditis elegans. *Development* 137:1657–1667.
51. Hong K, et al. (1999) A ligand-gated association between cytoplasmic domains of UNC5 and DCC family receptors converts netrin-induced growth cone attraction to repulsion. *Cell* 97:927–941.
52. Keleman K, Dickson BJ (2001) Short- and long-range repulsion by the Drosophila Unc5 netrin receptor. *Neuron* 32:605–617.
53. Killeen M, et al. (2002) UNC-5 function requires phosphorylation of cytoplasmic tyrosine 482, but its UNC-40-independent functions also require a region between the ZU-5 and death domains. *Dev Biol* 251:348–366.
54. Mortimer D, Fothergill T, Pujic Z, Richards LJ, Goodhill GJ (2008) Growth cone chemotaxis. *Trends Neurosci* 31:90–98.
55. von Philipsborn A, Bastmeyer M (2007) Mechanisms of gradient detection: A comparison of axon pathfinding with eukaryotic cell migration. *Int Rev Cytol* 263:1–62.
56. Tojima T, Hines JH, Henley JR, Kamiguchi H (2011) Second messengers and membrane trafficking direct and organize growth cone steering. *Nat Rev Neurosci* 12:191–203.
57. Farías GG, Guardia CM, De Pace R, Britt DJ, Bonifacino JS (2017) BORC/kinesin-1 ensemble drives polarized transport of lysosomes into the axon. *Proc Natl Acad Sci USA* 114:E2955–E2964.
58. Perrimon N, Pitsouli C, Shilo BZ (2012) Signaling mechanisms controlling cell fate and embryonic patterning. *Cold Spring Harb Perspect Biol* 4:a005975.
59. Lander AD (2013) How cells know where they are. *Science* 339:923–927.